NASA Technical Memorandum 104209

STS-40 ORBITAL ACCELERATION RESEARCH EXPERIMENT FLIGHT RESULTS DURING A TYPICAL SLEEP PERIOD

R. C. BLANCHARD

J. Y. NICHOLSON

J. R. RITTER

January 1992

NASA
National Aeronautics and
Space Administration

Langley Research Center
Hampton, Virginia 23665-5225

STS-40 ORBITAL ACCELERATION RESEARCH EXPERIMENT FLIGHT RESULTS DURING A TYPICAL SLEEP PERIOD

Robert C. Blanchard
NASA Langley Research Center
Hampton, Virginia 23665-5225

John Y. Nicholson
Vigyan , Inc.
Hampton, Virginia 23666-1325

James R. Ritter
Lockheed Engineering & Sciences Co.
Hampton, Virginia 23666-1339

Abstract

The Orbital Acceleration Research Experiment (OARE), an electrostatic accelerometer package with complete on-orbit calibration capabilities, was flown for the first time aboard Shuttle on STS-40. This is also the first time an accelerometer package with nano-g sensitivity and a calibration facility has flown aboard the Shuttle. The instrument is designed to measure and record the Shuttle aerodynamic acceleration environment from the free molecule flow regime through the rarified flow transition into the hypersonic continuum regime. Because of its sensitivity, the OARE instrument detects aerodynamic behavior of the Shuttle while in low-Earth orbit. A 2-hour orbital time period on day seven of the mission, when the crew was asleep and other spacecraft activities were at a minimum, was examined. During the flight, a "trimmed-mean" filter was used to produce high quality, low frequency data which was successfully stored aboard the Shuttle in the OARE data storage system. Initial review of the data indicated that, although the expected precision was achieved, some equipment problems occurred resulting in uncertain accuracy. An acceleration model which includes aerodynamic, gravity-gradient, and rotational effects was constructed and compared with flight data. Examination of the model with the flight data shows the instrument to be sensitive to all major expected low frequency acceleration phenomena; however, some erratic instrument bias behavior persists in two axes. In these axes, the OARE data can be made to match a comprehensive atmospheric-aerodynamic model by making bias adjustments and slight linear corrections for drift. The other axis does not exhibit these difficulties and gives good agreement with the acceleration model.

Nomenclature

A	=acceleration
Ap	=geomagnetic flux index
C	=aerodynamic force coefficient
C_a	=axial aerodynamic force coefficient
C_n	=normal aerodynamic force coefficient
C_y	=side-force aerodynamic force coefficient
$F_{10.7}$	=10.7 cm wavelength solar flux index
g	=gravitational acceleration at sea level (9.80665 m/s^2)
h	=altitude
M	=mass
MET	=mission elapsed time (i.e., time from lift-off)
nano-g	$=1x10^{-9}$ g
p, q, r	=body axes angular rates
$\dot{p}, \dot{q}, \dot{r}$	=body axes angular accelerations
S	=area
STS	=Space Transportation System
t	=time
T	=temperature
u, v, w	=air relative velocity body axes components
V	=velocity
V_a	=air relative velocity
X ,Y ,Z	=sensor axes
X_b ,Y_b ,Z_b	=body axes
X_s ,Y_s ,Z_s	=sensor location in the body axes
ρ	=density
ug	$=1x10^{-6}$ g

Subscripts

GG	=gravity-gradient
rot	=rotational
x,y,z	=component in x, y, and z directions

Introduction

The Orbital Acceleration Research Experiment (OARE) consists of a three axis, state-of-the-art accelerometer with an electrostatically suspended proof mass, a full in-flight calibration station, and a microprocessor which is used for in-fight experiment control, processing, and storage of flight data. The experiment system is purposely designed to measure low-frequency (<5 Hz), low-level acceleration (i.e., nano-g sensitivity) and is principally directed at characterizing the Orbiter's aerodynamic behavior in the rarefied-flow flight regime. An in-depth description of the experiment goals, equipment design characteristics, and capabilities is given in Ref. 1.

The first flight of the OARE was June 5, 1991 on the Shuttle mission, STS-40 which used the Columbia, i.e., Orbiter Vehicle (OV)-102. During the mission, data was collected over two time periods: (1) during launch and initial orbit insertion and (2) for a period of about 3.5 days beginning approximately 5.5 days after launch. The instrument was programmed to perform a calibration sequence approximately every hour. The calibration sequence includes up to nine separate bias calibrations (3 axes, 3 ranges) and up to six scale factor calibrations (2 table rates/axis, with y and z axes scaled simultaneously). A bias calibration consists of collecting 50 s of data in one position, rotating the sensor 180°, and then collecting data for another 50 s period. The sum of the average of each interval is twice the bias, while the difference is twice the average input signal. A scale factor calibration consists of rotating the sensor at a pre-programmed rate and measuring the acceleration difference between the sensor at rate and the average output at rest. This difference is scaled to the known centripetal acceleration which is a function of the square of the rate (which is measured) and the location of the sensor on the table (which is known). Two table rates are used for each sensor range for linearity checks.

The first flight of the OARE equipment has produced a wealth of information on making nano-g, low-frequency acceleration measurements, particularly with respect to the technology associated with calibrating in space. Some equipment problems, however, were noted on the first flight. Of particular importance was an apparent random bias shift which would occur after sensor motion was induced by the calibration table (and sometimes by the spacecraft). The magnitude of the shift was greatest in the sensor X-axis (on the order of 100 ug's) and least in the sensor Z-axis (on the order of a few ug's). After a shift, the accelerometer signal behaved as expected, namely, constant except for a slight linear drift. However, the sensor output occasionally exhibited erratic bias behavior for some period of time after a calibration. These sensor problems have introduced special considerations in the analysis of the

flight data in order to examine the flight measurements. This report provides the details of this analysis for a typical time period during which the orbiter crew was asleep. The time period selected was hours 16 to 18 on day 7, mission elapsed time. The principal reasons for this selection are: (1) Orbiter orientation: the aerodynamic acceleration would be directed mostly into the sensor Z axis (Orbiter Y_b axis) which exhibited the least erratic behavior throughout the entire mission and (2) background activity: during sleep periods, spacecraft activity (e.g., thruster firings) is significantly reduced.

Shuttle Location and Sensor Axes

The OARE system is mounted as a payload on the floor of the cargo bay on a keel-bridge spanning bay 11. The calibration table is composed of a dual gimbal platform. The proof mass is offset and aligned in such a way that rotation about two axes produces scale-factor calibrations for all three axes. During the data gathering periods of this flight, the table is set such that the sensor X axis is parallel to the Orbiter X body axis (X_b), the sensor Y axis is parallel to the Orbiter -Z body axis ($-Z_b$), and the sensor Z axis is parallel to the Orbiter Y body axis (Y_b) as depicted in Fig. 1. The approximate vector location of the sensor proof mass with respect to the Orbiter center of gravity in body coordinates during the 16 to 18 hour flight period of day 7 is (-1.666, -0.024, +1.376) meters.

Shuttle State Parameters

During the mission, measurements were taken by the Orbiter Project to determine the position, velocity and orientation vectors of the shuttle vehicle as a function of time, i.e., the vehicle state parameters. After the flight, the flight data information was disseminated to Shuttle experimenters. This section of the report discusses the STS-40 mission state parameters as flown during MET day 7, 16 to 18 hours.

Position and Velocity

Figure 2 shows the STS-40 mission orbit altitude and inertial and relative velocity variations on MET day 7 from 16 to 18 hours. As seen by the top graph, this time period includes an apogee to perigee to apogee variation. The complete orbital period is about 1.5 hours apogee to apogee. The near circular orbit provides an altitude variation of about 25 km and, based on the lower graphs in Fig. 2, the corresponding velocity variation is 30 m/s from apogee to perigee. The velocity

denoted by a solid line is the velocity relative to the air assuming the entire atmosphere is rotating with the Earth at altitude. This is the velocity important to the aerodynamic behavior of the Orbiter discussed later. A decrease in altitude is accompanied by an increase in density and corresponding increase in velocity which combine to produce a small change (increase) in acceleration due to aerodynamics. A rough estimate of the increase in aerodynamic acceleration for this orbit is about 125 nano-g based upon the 1976 U.S. Standard Atmosphere[2], the STS-40 mass to area ratio, and a constant Orbiter's free molecule aerodynamic force coefficient of 2.0. However, typically the Orbiter's orientation is not constant and, therefore, the coefficients are not constant. The proper behavior of the anticipated acceleration levels requires examining the orientation component of the vehicle state vector which is discussed next.

Shuttle Orientation

The analysis of the OARE flight data in this report concentrates on the Shuttle crew sleep period on day seven after launch. Figure 3 illustrates the approximate orientation of the Orbiter during the selected data collection period, namely, the right wing of the Orbiter is placed nearly into the velocity vector, while the nose is directed toward Earth (a stable gravity-gradient orientation). The top graph in Fig. 4 shows the actual orientation of the Orbiter during the time of interest in terms of angle-of-attack, α and side-slip angle, β. As seen in Fig. 4, the velocity vector is not entirely into the right wing. Side-slip angle varies from about 40 to 90 degrees. Near $\beta=90^{o}$, with α nearly 90^{o}, an apparent abrupt change in α occurs as the velocity vector changes from impinging on the belly to impinging on the top of the Orbiter due to a slight change in the orientation of the right wing. [Note: The common practice of considering angle of attack in terms of pitch and sideslip in terms of yaw, while acceptable for normal atmospheric flight, is misleading for interpreting Shuttle orbital orientations. Rather, recall the definitions[3] of each term, $\alpha = \tan^{-1}(w/u)$ and $\beta = \sin^{-1}(v/V_a)$ where u, v, and w are body axes wind speed components and V_a is wind speed magnitude.]

The bottom of Fig. 4 shows the corresponding values of the body axes aerodynamic coefficients from the Orbiter aerodynamics data base[4]. These coefficients correspond to the upper figure relative velocity wind angles using a bivariate interpolation of the data base. The coefficients provided by the Orbiter Project assume complete thermal accommodation in the free molecule flow region and are the current best estimates.

Acceleration Model

An acceleration model which accounts for the major low frequency components of orbital acceleration has been generated and compared with flight data. This analysis approach has been taken due to the uncertain nature and reliability of the OARE equipment on its first flight, STS-40. The model includes "as measured" STS-40 orbital and orientation parameters during the time of interest (i.e., MET 7^d, 16 to 18 hours) previously discussed. The model used in the analysis includes components of free-molecule flow aerodynamics, gravity-gradient, and rotational terms. A discussion of each is given in the next sections.

Aerodynamics

The body axes acceleration vector components (m/s^2) due to aerodynamics are

$$A_i = 1/2\ \rho\ V_a^2\ (S/M)\ C_i \qquad \text{where i=x, y, or z.}$$

Coefficient C_i is related to the body axis aerodynamic coefficients by

$$C_x = -C_a\ ,$$
$$C_y = C_y\ \text{, and}$$
$$C_z = -C_n\ ,$$

ρ is the air density(kg/m^3), V_a is the air relative velocity (m/s), S is the coefficient reference area ($249.909 m^2$), and M is the orbiter weight which is 107,777.2 kg for this application.

Two sources of air density are used in the aerodynamic calculations, namely, the 1976 U.S. Standard Atmosphere model[2] and the Hedin model[5], which unlike the 1976 model, includes effects of local solar time, solar cycle, etc. Figure 5 shows the results of the density variation in time for both models for the STS-40 mission as flown. The 1976 model only depends on altitude and thus the variation seen results from the change of Orbiter's altitude from apogee to perigee. However, the Hedin model includes in addition, both latitude and longitude (i.e., time of day) effects as well as solar cycle ($F_{10.7}$ index of 80) and geomagnetic effects (geomagnetic index Ap of 4). Both $F_{10.7}$ and Ap are moderate values.

The results of the calculations of the expected body axes aerodynamic accelerations for the two atmosphere models are shown in Fig. 6. The air relative

velocity and the aerodynamic coefficients used are those previously discussed which are derived from the state vector as flown on STS-40. It can be seen from Fig. 6 that the atmosphere models chosen (1976 U.S. Standard or Hedin) influence the acceleration much more in the Y_b-axis than in either of the other two axes. This is expected since both the X_b-axis and the Z_b-axis are more nearly normal to the velocity vector than is the Y_b-axis during this interval of time, and therefore, the acceleration seen in either the X_b- or Z_b- axis direction would be influenced greatly by the exact Orbiter orientation. Consequently, for the time period under examination, only the Y_b-axis acceleration data could be expected to be indicative of the atmospheric model.

Gravity-Gradient Terms

A low-frequency non-aerodynamic acceleration signal which affects the sensor is that produced by the "gravity-gradient" effect. The magnitude of this effect is a function of the orientation of the vector from the Orbiter's center of gravity (c.g.) to the OARE sensor relative to the local vertical. For instance, if the sensor is below the Orbiter's c.g., the proof-mass will be accelerated toward the Earth relative to the c.g. If the sensor is above the c.g., then the proof-mass will be accelerated away from the Earth relative to the c.g. Thus, the gravity-gradient effect vector is directed along the c.g., to the center of the Earth line. For the OARE location, and assuming a circular orbit, the gravity-gradient effect on the sensed acceleration is,

$$A_{GG} = -0.276\,\Delta r \qquad \text{(ug)}$$

where Δr is the difference in height from the Orbiter c.g., to the OARE sensor (m). The assumption of circular orbit introduces an error of less than about 8 nano-g in the predominant axis, X_b. The components of acceleration in the body axes induced in the OARE sensor depend on the direction of the Orbiter relative to local vertical. This orientation, in terms of direction cosines, is given by the STS-40 data. Applying the orientation as-flown culminates in the acceleration components as shown in Fig. 7. Only the X_b-axis is a significant contributor relative to the aerodynamics for this nose-down configuration, for which the gravity-gradient effect is more than twice the aerodynamic effect.

Rotational Terms

Another non-aerodynamic contributor to the sensor signal is the rotation of the sensor about the Orbiter's c.g. The rotational acceleration components (m/s^2) is given as[5],

$$\begin{bmatrix} a_{X\,rot} \\ a_{Y\,rot} \\ a_{Z\,rot} \end{bmatrix} = \begin{bmatrix} -(q^2 + r^2) & pq - \dot{r} & pr + \dot{q} \\ pq + \dot{r} & -(p^2 + r^2) & qr - \dot{p} \\ pr - \dot{q} & qr + \dot{p} & -(q^2 + p^2) \end{bmatrix} \begin{bmatrix} X_S \\ Y_S \\ Z_S \end{bmatrix}$$

where X_S, Y_S, Z_S are the OARE sensor coordinates (m) relative to the Orbiter c.g. and p,q,r (s^{-1}) and $\dot{p}$, $\dot{q}$, $\dot{r}$ (s^{-2}) are the angular velocity and acceleration about the body axes, respectively. For the STS-40 mission, the body angular rates are part of the postflight mission data set and are shown in Fig. 8. The angular accelerations are very small in comparison to measured angular velocities. Figure 9 shows the results of the calculations. Here again, there is a large contribution in the X-axis which is mostly due to the sensor lever arm distance and large magnitude of r and q relative to p.

Other Terms

Other effects such as solar radiation pressure, Coriolis force, and out-of-plane contributions were considered for the model, but their contributions were found to be too small for the present initial analysis.

Combined Components

Figure 10 shows the combined effect of all the acceleration model components for all three axes. The aerodynamics derived from the Hedin atmosphere model is labeled "aero" in the figure. The curves labelled "GG" and "rot" are the gravity-gradient and rotational effects, respectively. The major contributions to the X_b-axis signal in the order of significance are gravity-gradient, rotational effects, and then aerodynamics. However, for the Y_b and Z_b axes, the aerodynamic signal is dominant, as expected. The role of the other two acceleration terms are to slightly shape the Y_b and Z_b signals. Note, the X_b-axis ordinate scale is different than that of the other two axes. Figure 11 is a graph of the total acceleration for all three axes on the same scale in order to properly view the signals of each axis relative to one another.

Shown in Fig. 11 are what a properly operating low-frequency Orbiter acceleration system should measure in this time frame. Namely, the X_b-axis is predominantly a straight line and slightly positive (about 0.7 ug) dominated by non-aerodynamic inputs. The Z_b-axis is the largest varying signal due to a significant

change in Orbiter orientation during the interval. The Y_b-axis shows the next largest variation mostly caused by orbit changes, i.e., due to atmosphere variations from apogee to perigee. This axis magnitude could readily be shifted up or down pending the actual atmosphere encountered during flight. Note the phase difference between the Y_b and Z_b signals indicating the source of the input. This model will be used to compare the measured signals of the OARE sensor during this time interval which is discussed next.

Flight Data Analysis

Trimmed-Mean Filter

For STS-40 a trimmed-mean filter has been programmed in the OARE processor. This filter is directed at the low frequency aerodynamic component of the acceleration measurements. A trimmed-mean filter was selected for its effectiveness in providing a measurement average without being affected by wild points or thruster firings. A brief description of the algorithm is as follows. First, data in a data window is ordered, low to high value. Then, a "quality index" is calculated based upon the data distribution. A large magnitude of the quality index denotes greater scatter of the data points, for instance, to noise spikes or thruster activity. From the quality index, a quantity "alpha" is calculated which can range in value from about 0.05 to 0.40. Alpha is the portion of the entire ordered data set to be removed from the low and high end. Upon removal, the data remaining is then simply averaged. Testing has shown this algorithm to be very effective in producing a meaningful average in the presence of spurious data.

Data Rates

Internally, the OARE processes the sensor signals at the rate of 20 per second. Two sequential measurements are averaged with a simple analog filter producing an effective raw data sampling rate of 10 per sec. For the first flight, a trimmed-mean filter window of 50 s was used. Thus, each processed data point represents data averaged over 50 s. The window slides by 25 s is so that the next processed data point shares some data with the preceding point and the sample rate is now 1 every 25 s. These trimmed-mean filter processed data are used in the analysis of the acceleration discussed in this report.

Flight and Model Comparisons

The X_b, Y_b, and Z_b axes OARE processed flight data are shown in Figs. 12, 13, and 14, respectively (note the difference in scales). The gap in the flight data is the time during which calibrations are being performed. Just prior to and after the data shown are also calibrations time periods. The calibration data are analyzed separately for bias and scale factors. The bias factors determined by the in-fight calibration have been applied to the data labeled "flight." Clearly, as previously discussed, the X_b- and Z_b- axis accelerations exhibit the shift problem which appears after a calibration. Also seen on these axes are the effects of the destabilized sensor attempting to settle down after an apparent reset (note the right-hand side of Figs. 12 and 14). However, the Y_b-axis does not appear to have the same difficulties. Also shown on each graph is the corresponding acceleration model results (i.e., Fig. 11). By arbitrarily adjusting the bias and allowing for a linear term, both X_b and Z_b flight data can match the basic predicted Orbiter environment behavior. These curves are labeled "adjusted." The Y_b-axis shown is the in-flight data as measured (without scale factor adjustment) and compares well with the model. Recall that this axis is strongly dependent on the atmosphere, and thus, the aerodynamics.

Summary

A detailed analysis of the low frequency acceleration experienced by the Orbiter on STS-40 during a segment of a typical sleep period (on MET 7^d 16-18 hours) has been performed in order to investigate the viability of the OARE flight data. An elaborate model with major components of the low frequency acceleration has been generated in order to compare with the OARE flight measurements. The acceleration model includes three components: aerodynamic, gravity-gradient, and rotational effects. The "as flown" state parameters (i.e., position, velocity, and orientation vectors) are used to predict the OARE measurements with the model. The aerodynamic acceleration predictions use the free molecule flow, fully accommodated preflight body axes aerodynamic coefficients. Two atmosphere models (1976 U.S. Standard and Hedin) have been examined. The low frequency total accelerations which are generated by each model along the body axes indicate a complex nature where magnitude, phase and frequency are strongly dependent upon state parameters and atmosphere conditions, as expected. A comparison of the predictions from the acceleration model with the corresponding OARE flight measurements indicates: (1) the Y_b-axis (Z sensor axis) appears to be working, (2) the Y_b-axis bias calibration also appears to be working, (3) the X_b and Z_b axes (X and Y sensor axes) are not working

properly, although some reasonable adjustments do provide the correct character of the relative signal (after calibration transients dissipate). In addition, it appears that a Hedin atmosphere model with low-to-moderate solar activity is close to the actual flight conditions predicted by the Y_b axis accelerometer at the time of measurements. The instrument will clearly require adjustments and refurbishment prior to the next flight to improve Y_b measurements and restore the X_b and Z_b measurements to their design capabilities.

Acknowledgments

The authors would like to include a list of the various people and their respective organizations without whom the experiment could not have been possible. However, this list is indeed too lengthy. We will acknowledge instead the Orbiter Experiment (OEX) Project Office, at NASA Johnson Space Center, who were invaluable in the execution of this experiment. They supervised the construction and testing of OARE, integrated OARE objectives into the STS-40 flight plan, and processed raw telemetered OARE data into computer compatible tapes for use by the principal investigator.

References

[1]Blanchard, R.C., Hendrix, M.K., Fox, J.C., Thomas, D.J., and Nicholson, J.Y., "The Orbital Acceleration Research Experiment," Journal of Spacecraft and Rockets, Vol. 24, No. 6, Nov.-Dec. 1987, pp. 504-511.

[2]U.S. Standard Atmosphere, 1976, NOAA, NASA, USAF, Oct. 1976.

[3]Etkin, Bernard, Dynamics of Atmospheric Flight, John Wiley and Sons, Inc., New York, 1972, page 114.

[4]Aerodynamics Design Data Book-Vol. I: Orbiter Vehicle, NASA CR-160386, 1978.

[5]Hedin, A. E., "A Revised Thermospheric Model Based on Mass Spectrometer and Incoherent Scatter Data: MSIS-83," Journal of Geophysical Research, Vol. 88, December 1983, pp. 10170-10188.

[6]Blanchard, R. C. and Rutherford, J. F., "Shuttle Orbiter High Resolution Accelerometer Package Experiment: Preliminary Flight Results," Journal of Spacecraft and Rockets, Vol. 22, No. 4, Jul-Aug. 1985, pp. 474-480.

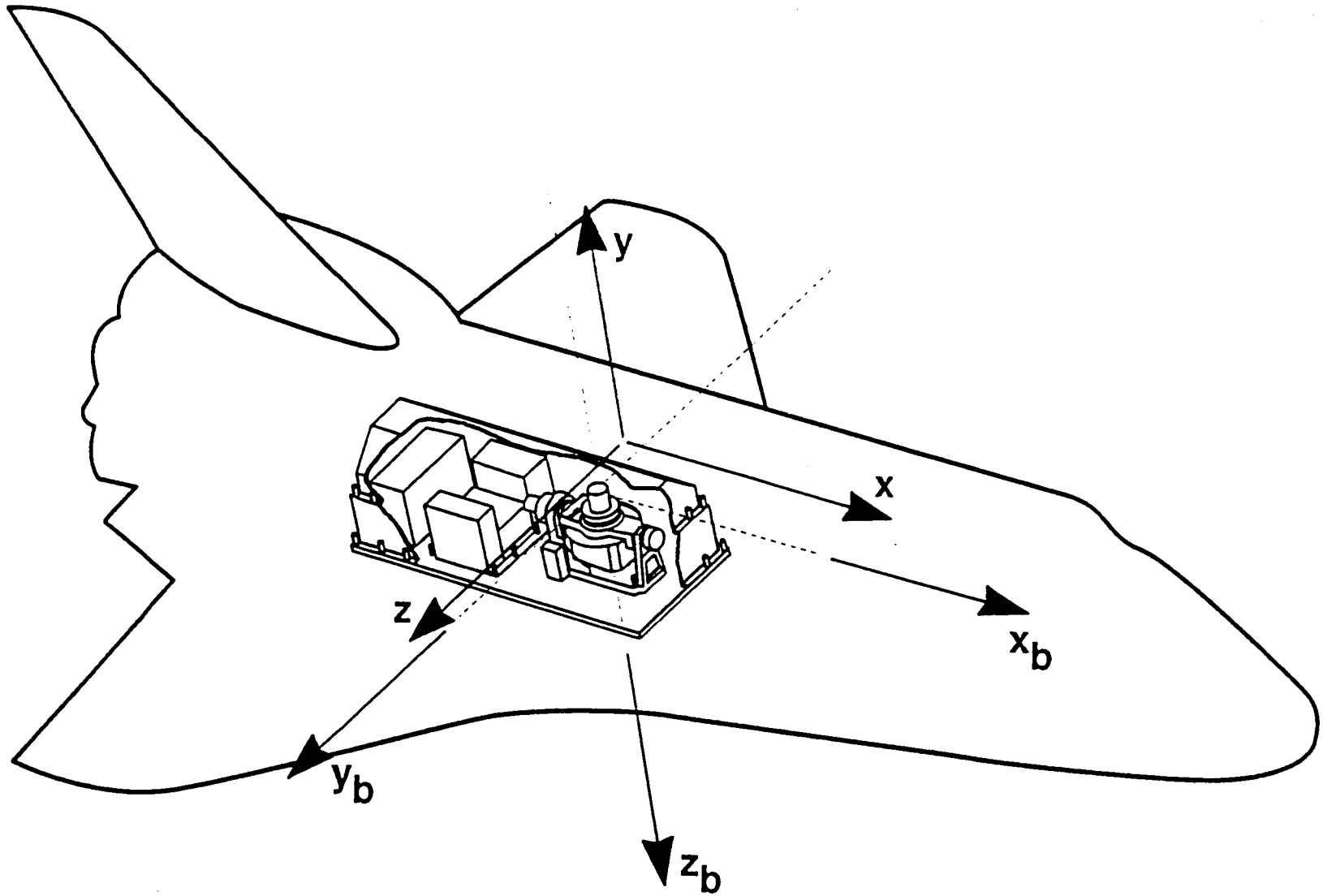

Figure 1. OARE/Shuttle Axes Relationships during data collection.

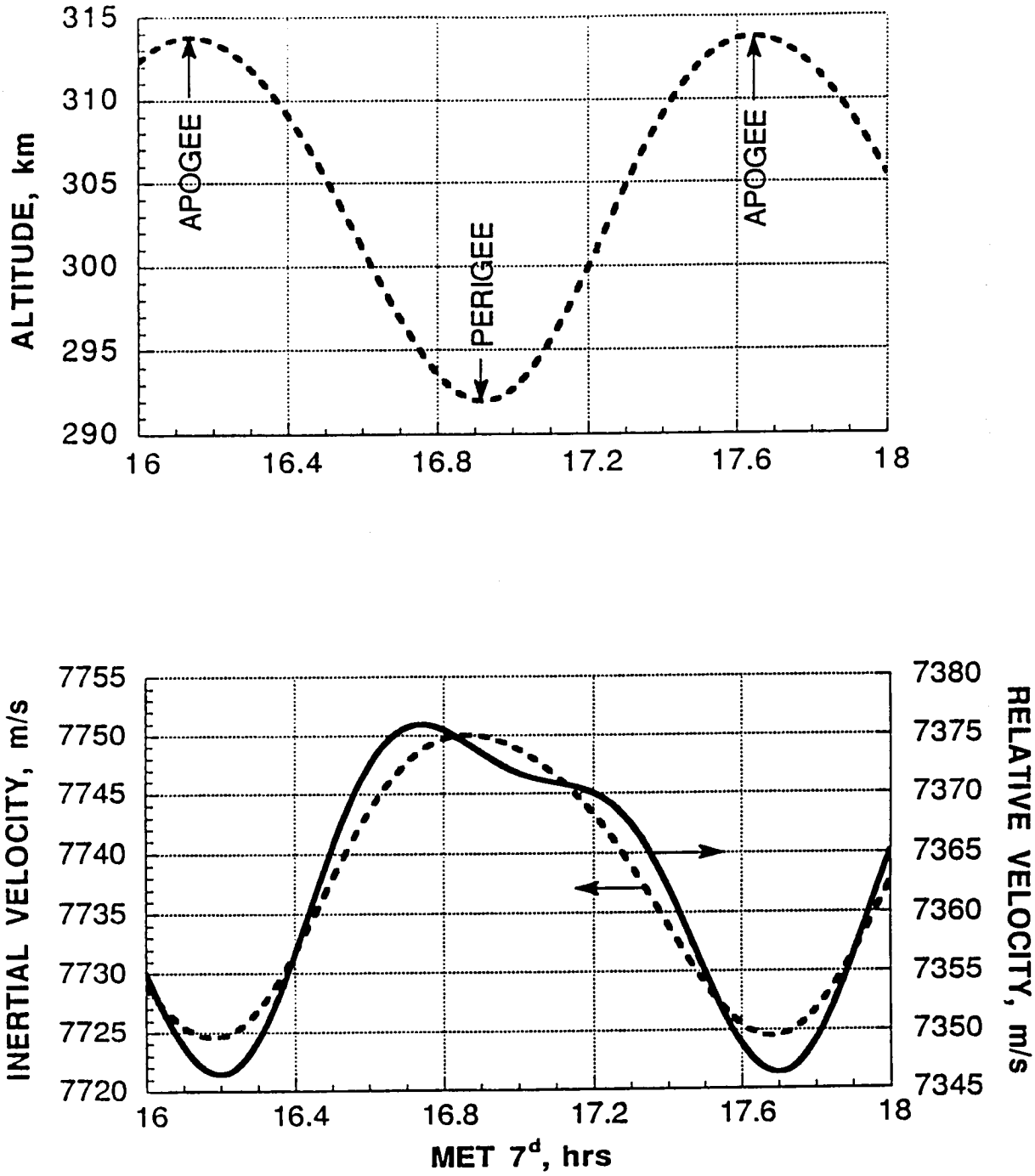

Figure 2. Shuttle Altitude and Velocity Time History.

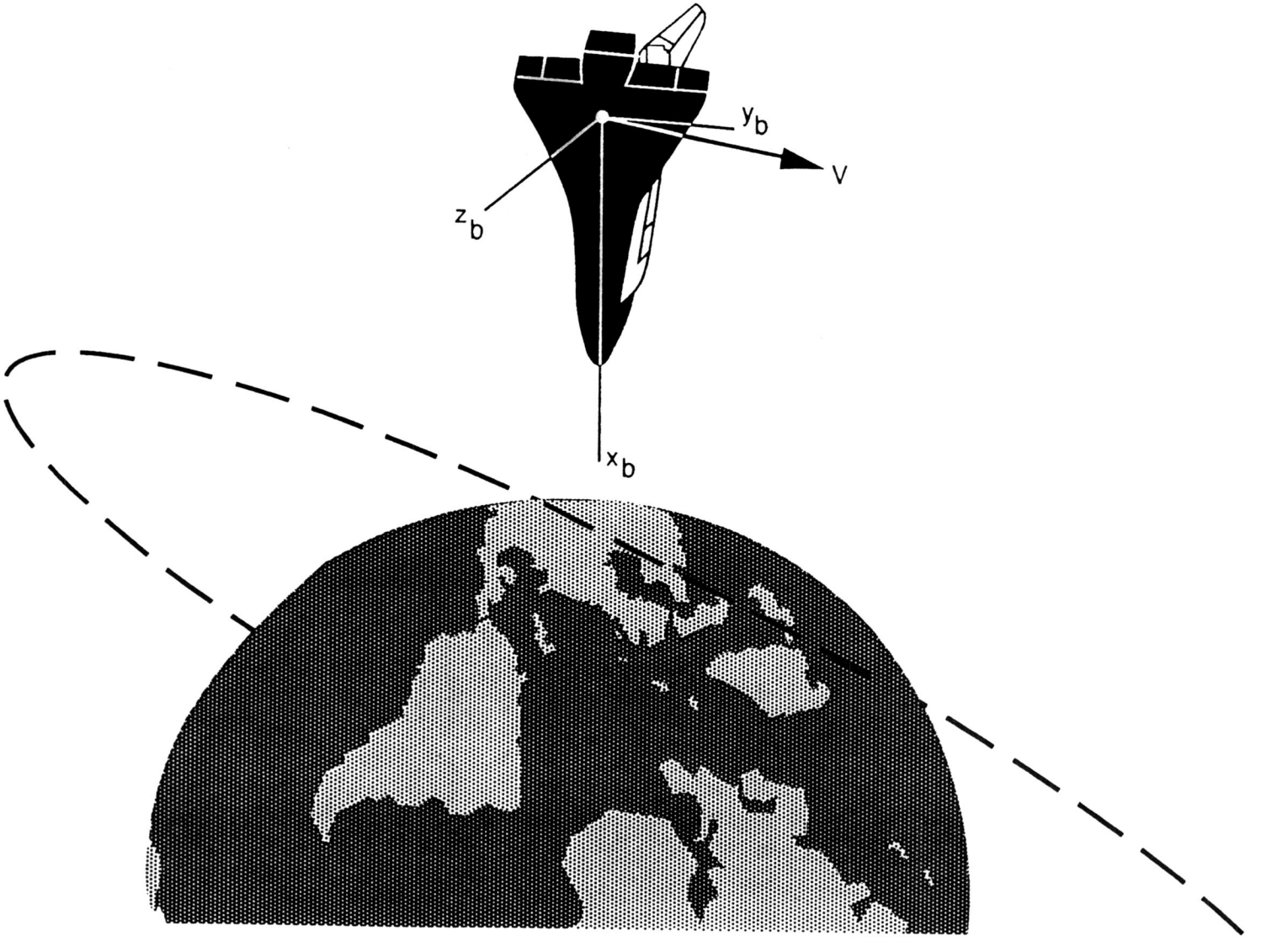

Figure 3. Approximate Orbiter Orientation during OARE Analysis.

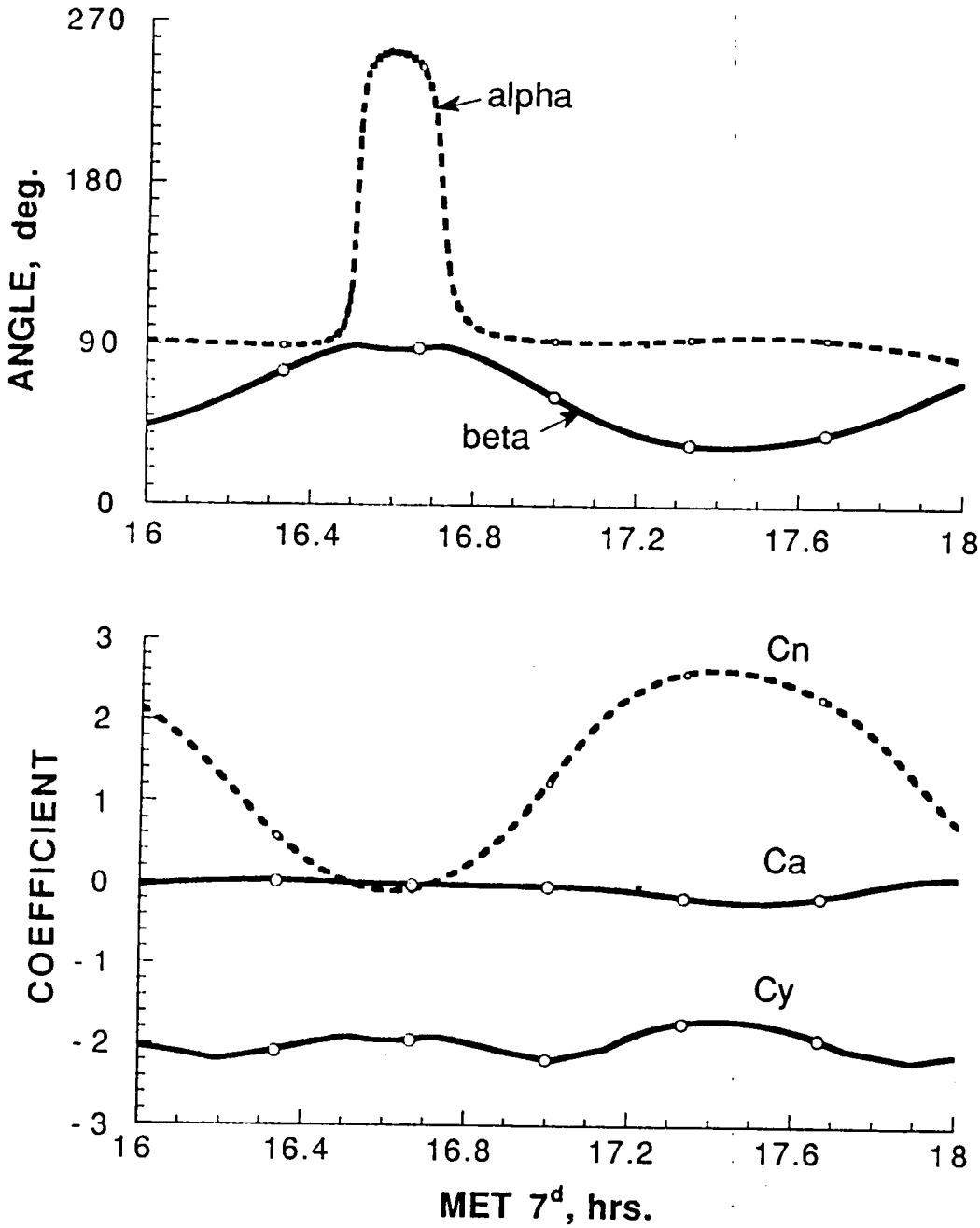

Figure 4. Orbiter Aerodynamic Angles (a) and Body Axis Coefficients (b).

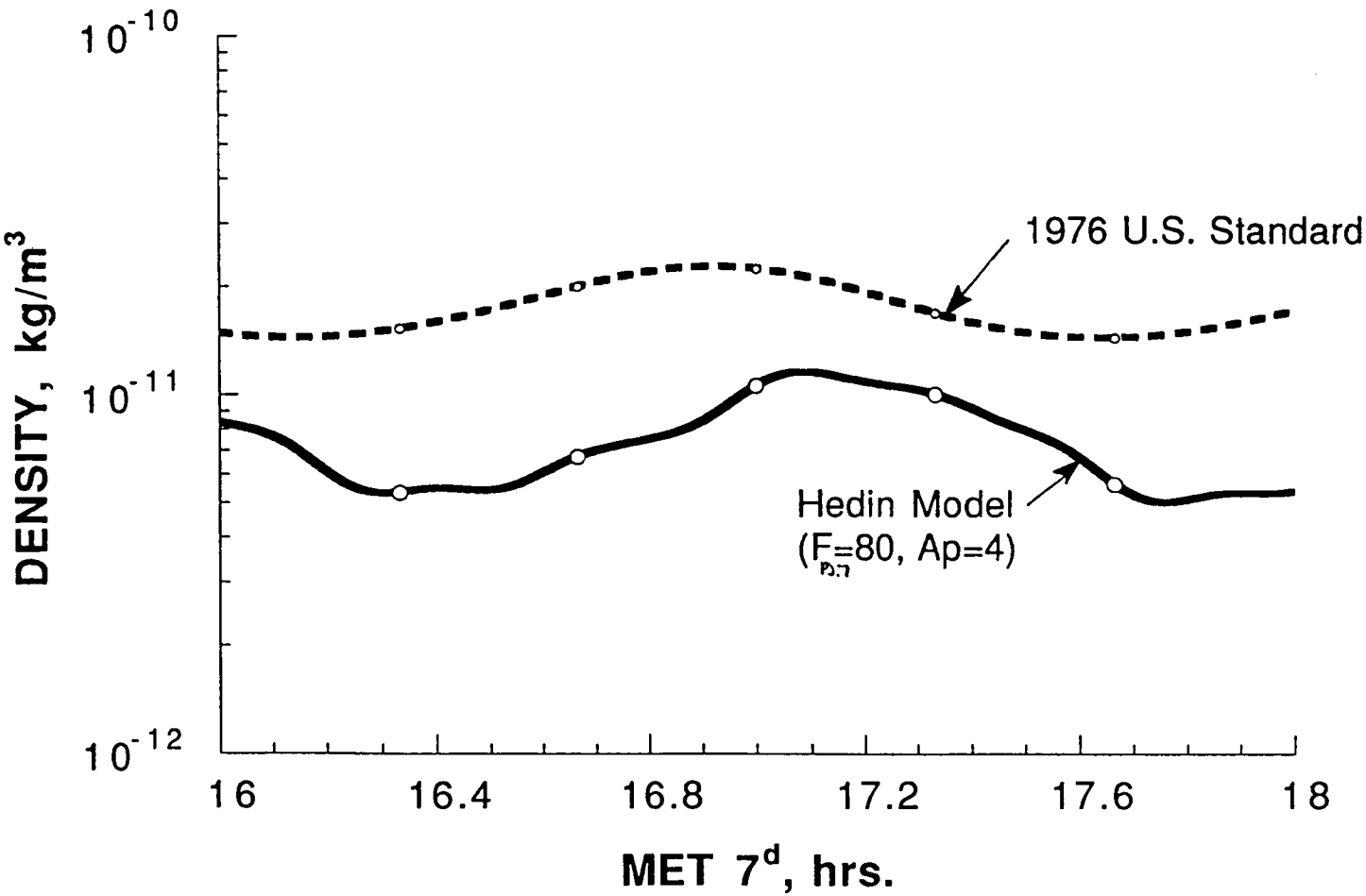

Figure 5. Atmospheric Density Models.

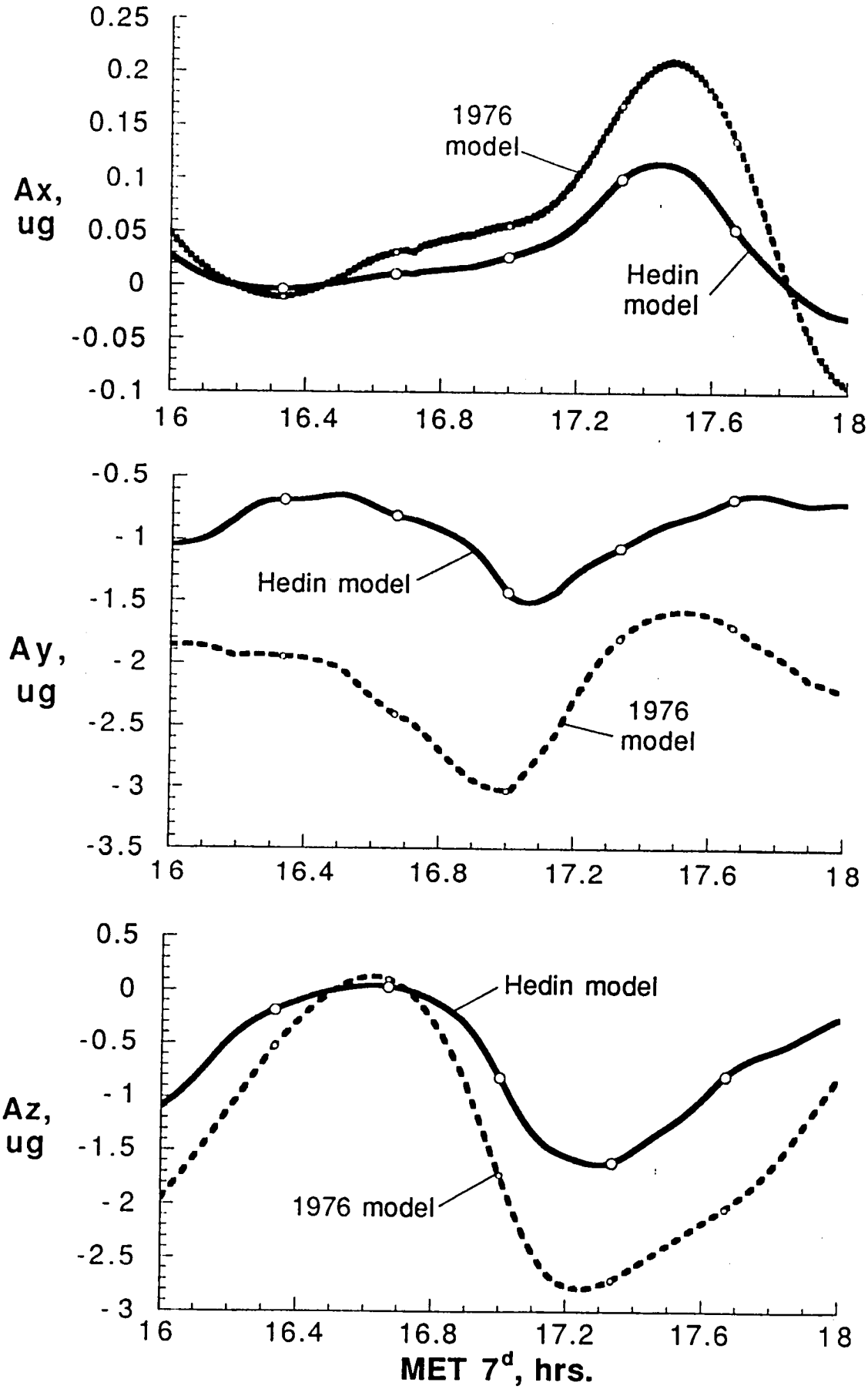

Figure 6. Body Axes Aerodynamic Accelerations calculated from Density Models.

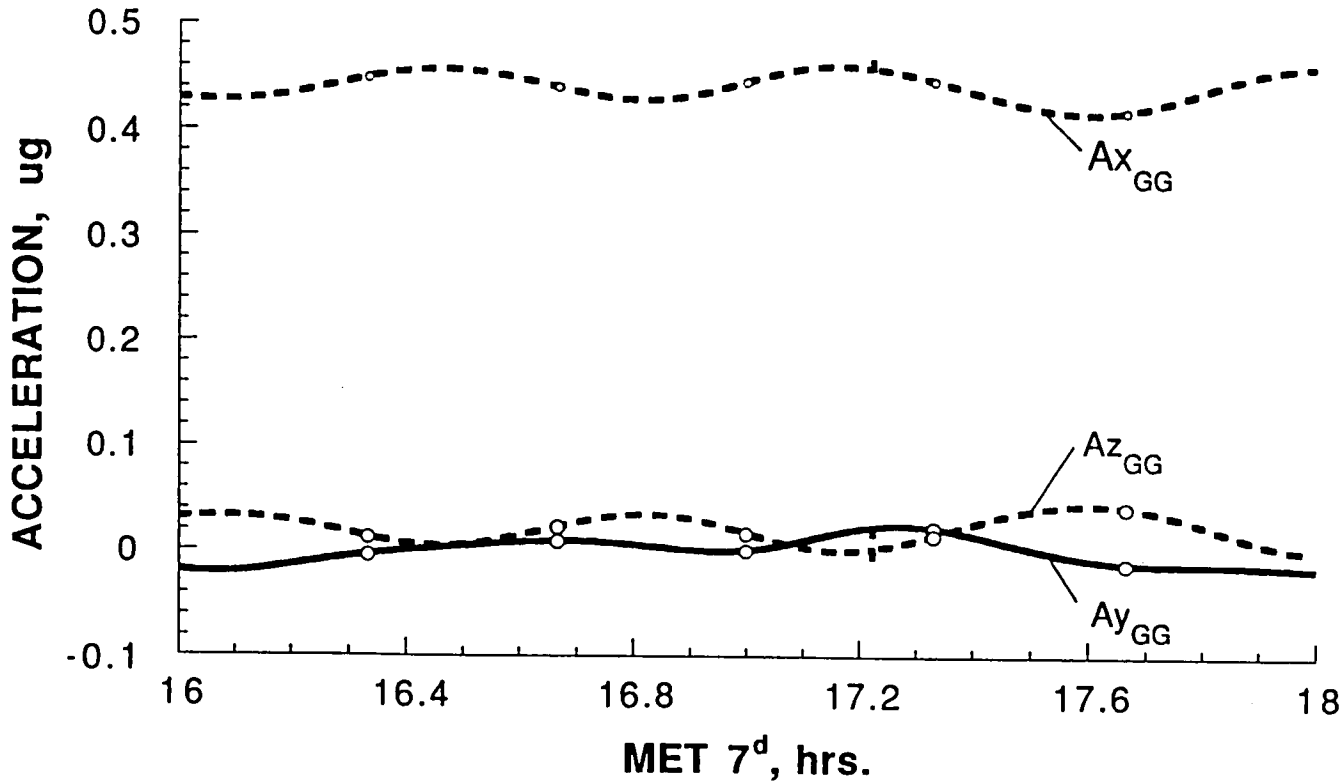

Figure 7. Body Axes Acceleration Components due to the Gravity Gradient Effect.

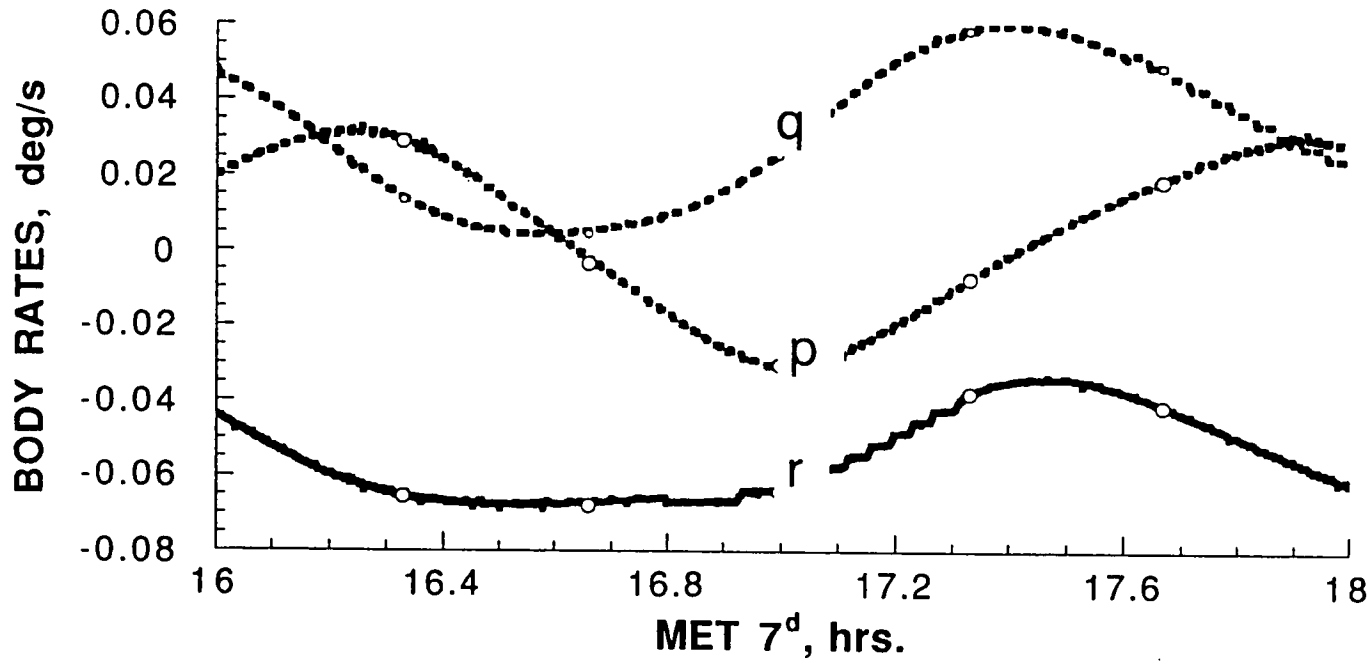

Figure 8. Orbiter Angular Velocities about Body Axes.

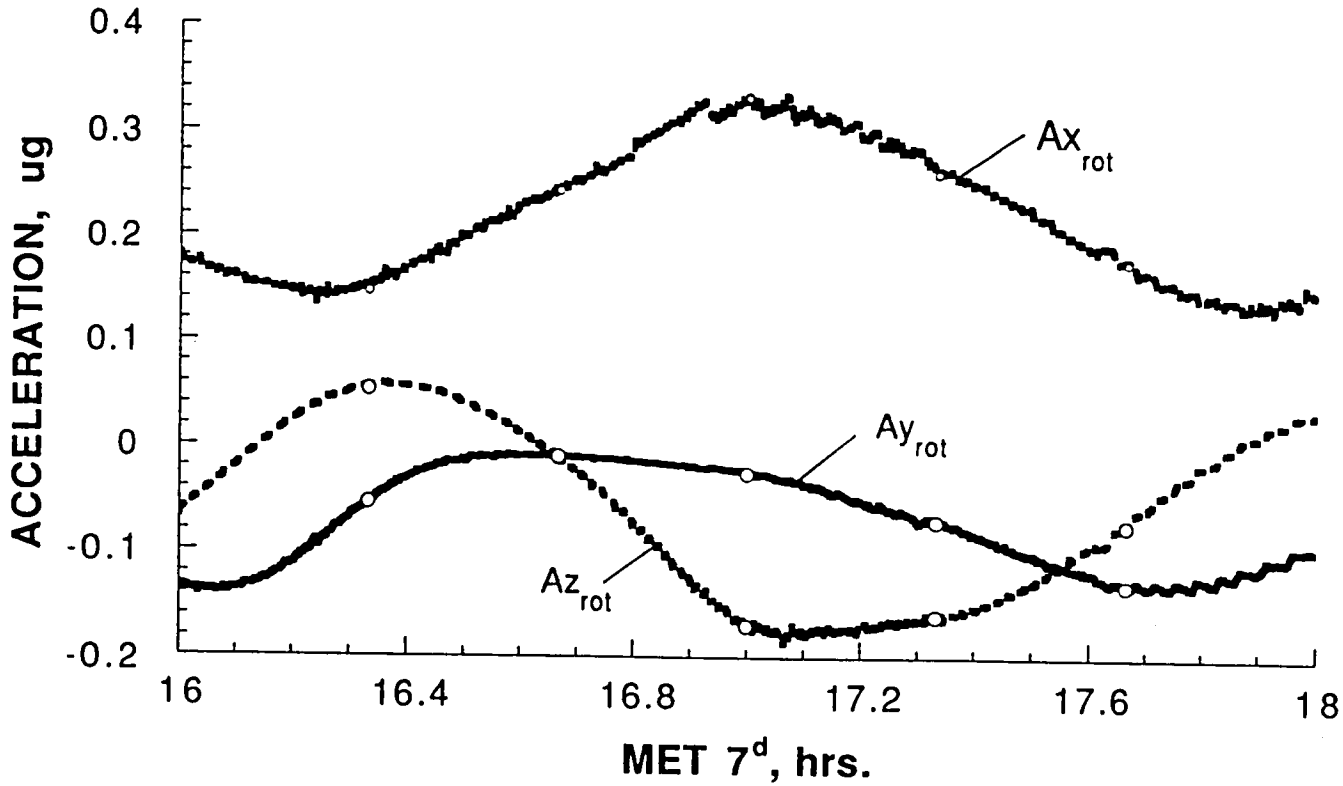

Figure 9. Rotation Induced Accelerations in the Orbiter Body Axes at the OARE Location.

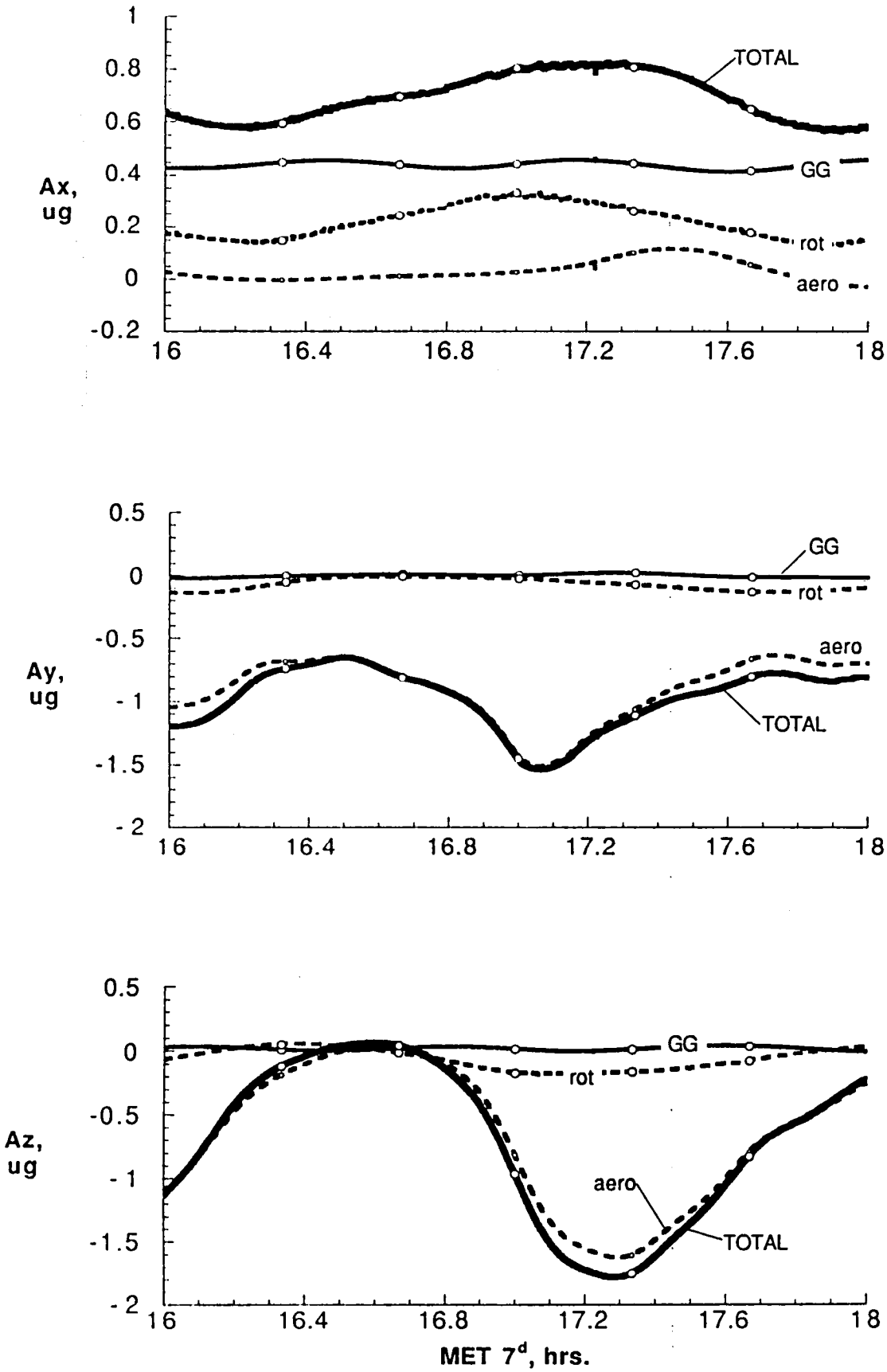

Figure 10. Body Axes Acceleration Constituents using the Hedin Atmospheric Model.

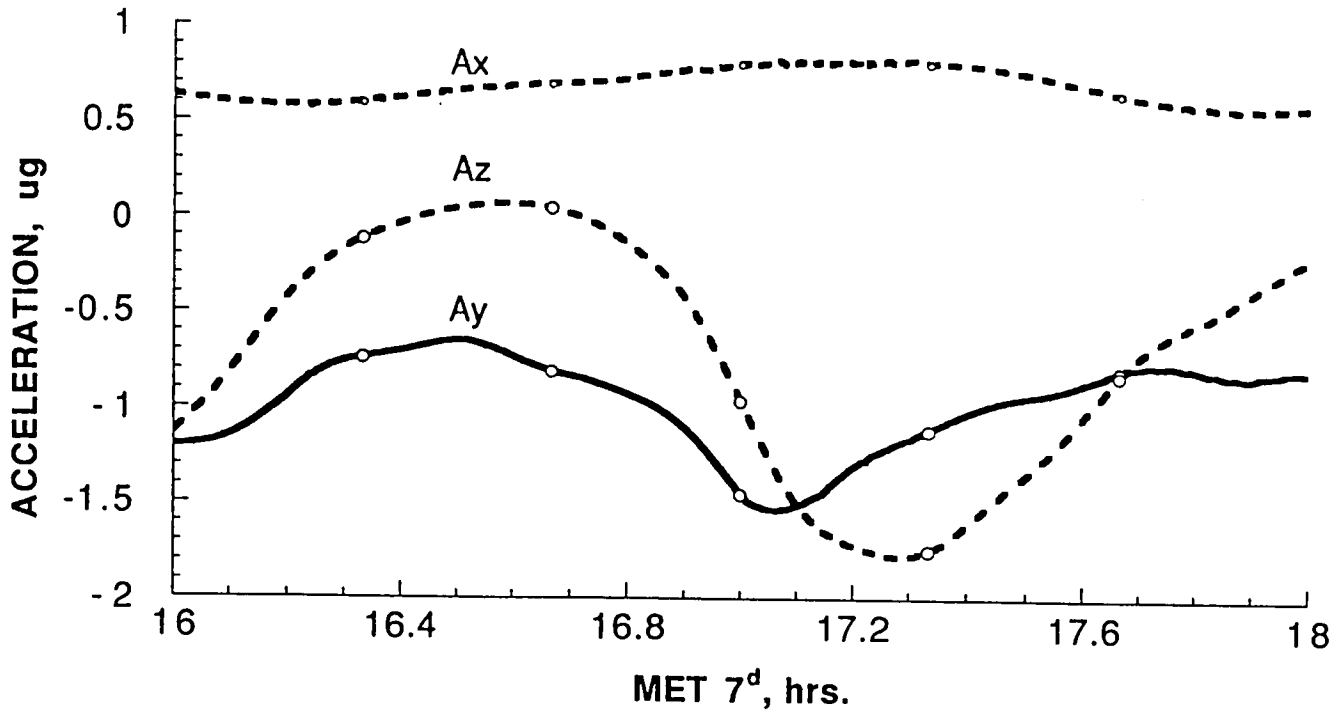

Figure 11. Total Calculated Accelerations at the OARE Sensor Location using the Hedin Atmospheric Model.

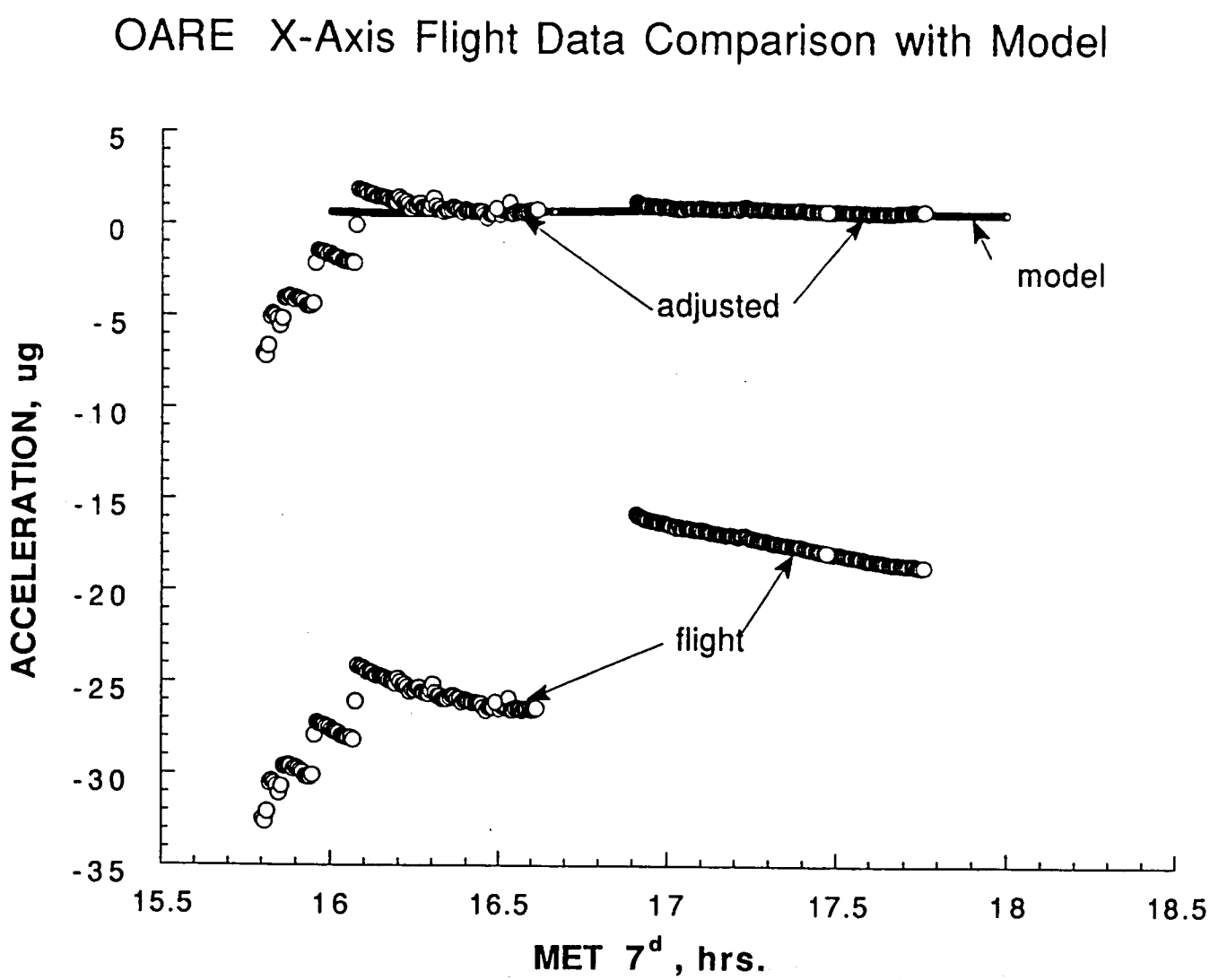

Figure 12. OARE X-Axis Flight Data Compared with Calculated Model.

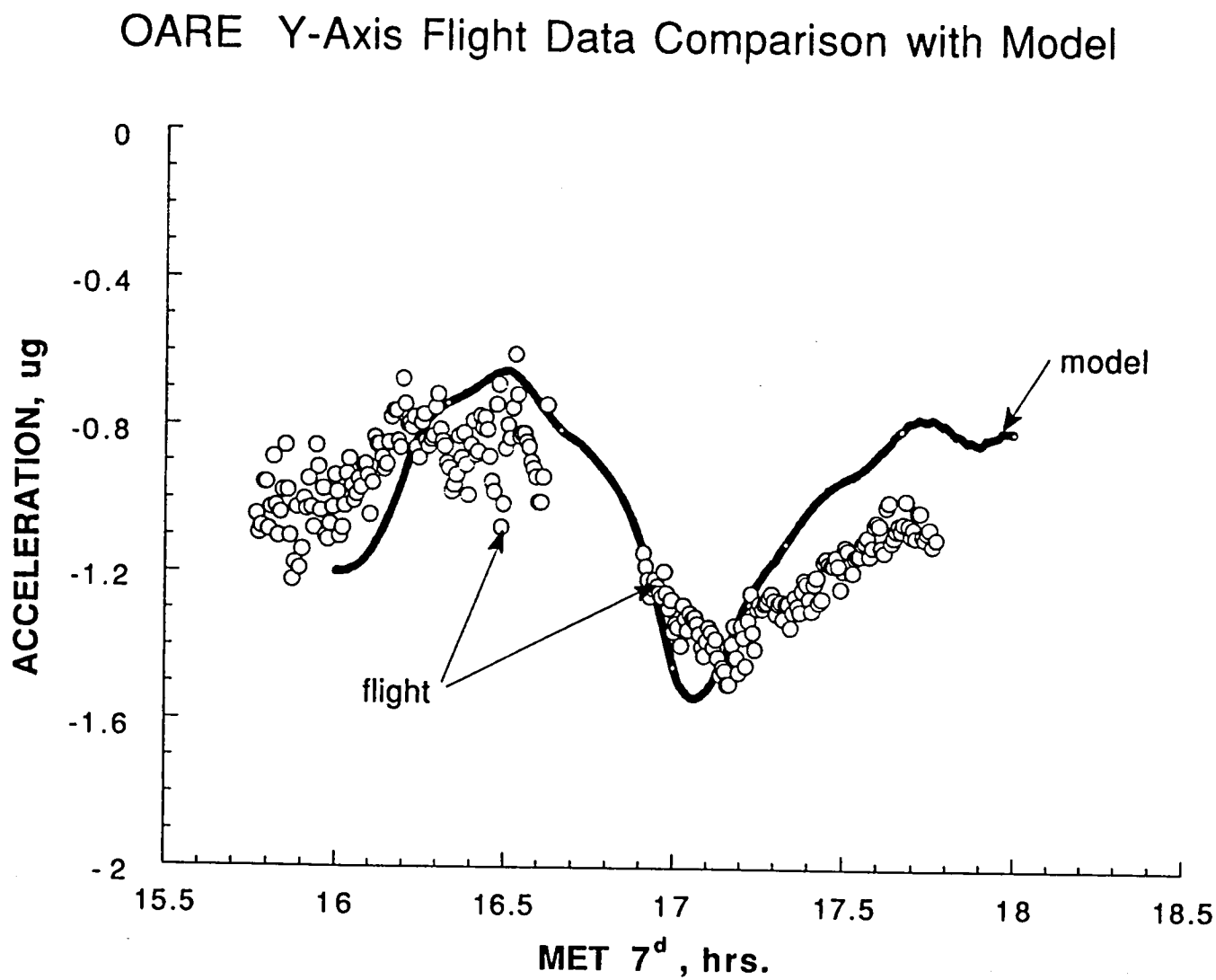

Figure 13. OARE Y-Axis Flight Data Compared with Calculated Model.

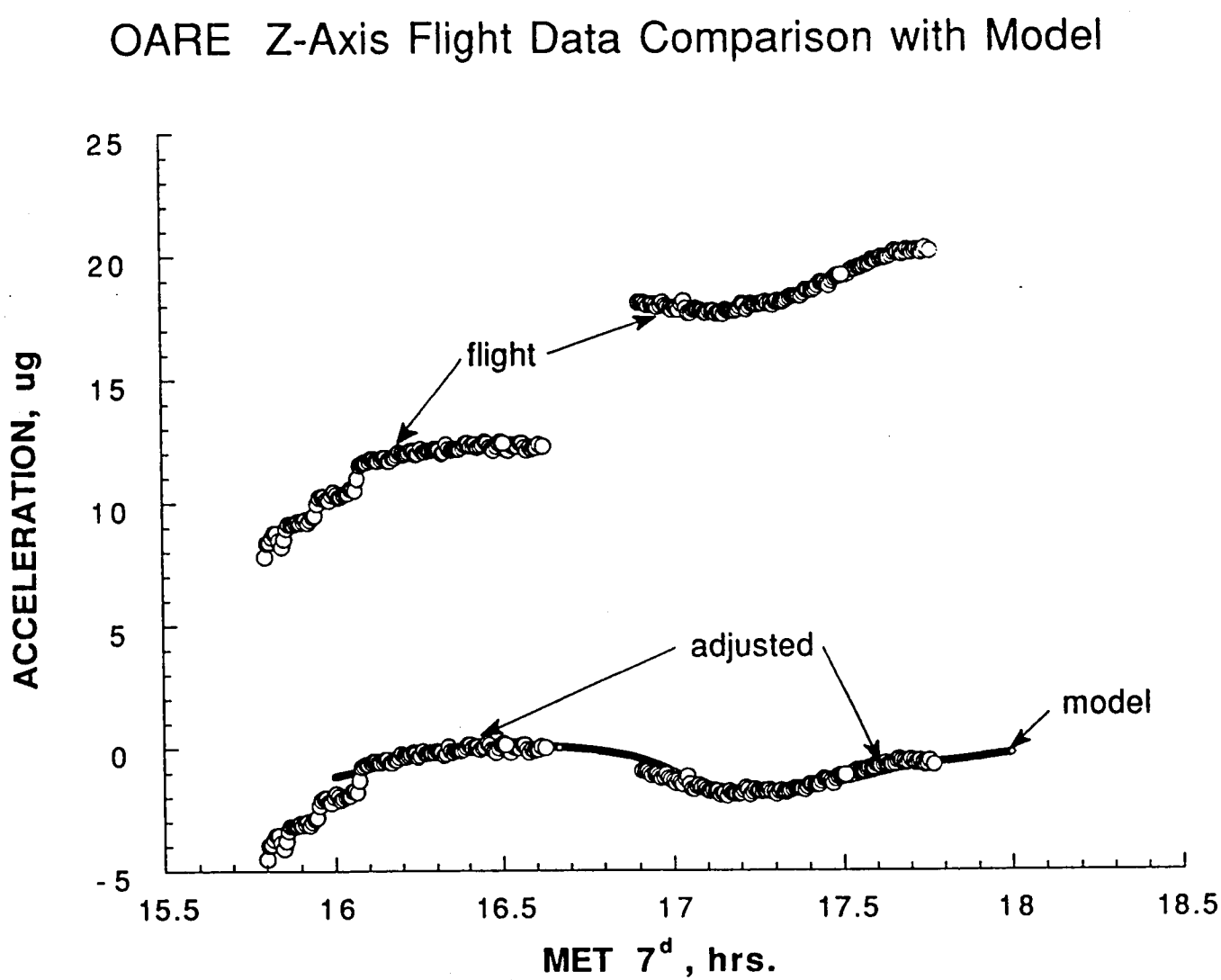

Figure 14. OARE Z-Axis Flight Data Compared with Calculated Model.

REPORT DOCUMENTATION PAGE

Form Approved
OMB No. 0704-0188

1. AGENCY USE ONLY *(Leave blank)*	2. REPORT DATE	3. REPORT TYPE AND DATES COVERED
	January 1992	Technical Memorandum

4. TITLE AND SUBTITLE
STS-40 Orbital Acceleration Research Experiment Flight Results During a Typical Sleep Period

5. FUNDING NUMBERS
WU 506-48-11-05

6. AUTHOR(S)
R. C. Blanchard, J. Y. Nicholson, and J. R. Ritter

7. PERFORMING ORGANIZATION NAME(S) AND ADDRESS(ES)
NASA Langley Research Center
Hampton, VA 23665-5225

8. PERFORMING ORGANIZATION REPORT NUMBER

9. SPONSORING/MONITORING AGENCY NAME(S) AND ADDRESS(ES)
National Aeronautics and Space Administration
Washington, DC 20546-0001

10. SPONSORING/MONITORING AGENCY REPORT NUMBER
NASA TM-104209

11. SUPPLEMENTARY NOTES
R. C. Blanchard: Langley Research Center, J. Y. Nicholson: Vigyan, Inc., and J. R. Ritter: Lockheed Engineering & Sciences Co.

12a. DISTRIBUTION/AVAILABILITY STATEMENT
Unclassified-Unlimited
Subject Category 34

12b. DISTRIBUTION CODE

13. ABSTRACT *(Maximum 200 words)*

The Orbital Acceleration Research Experiment (OARE), an electrostatic accelerometer package with complete on-orbit calibration capabilities, was flown for the first time aboard Shuttle on STS-40. The instrument is designed to measure and record the Shuttle aerodynamic acceleration environment from the free molecule flow regime through the rarified flow transition into the hypersonic continuum regime. Because of its sensitivity, the OARE instrument detects aerodynamic behavior of the Shuttle while in low-Earth orbit. A two-hour orbital time period on day seven of the mission, when the crew was asleep and other spacecraft activities were at a minimum, was examined. An acceleration model which includes aerodynamic, gravity-gradient, and rotational effects was constructed and compared with flight data. Examination of the model with the flight data shows the instrument to be sensitive to all major expected low-frequency acceleration phenomena; however, some erratic instrument bias behavior persists in two axes. In these axes, the OARE data can be made to match a comprehensive atmospheric-aerodynamic model by making bias adjustments and slight linear corrections for drift. The other axis does not exhibit these difficulties and gives good agreement with the acceleration model.

14. SUBJECT TERMS
Free-molecular, aerodynamics, gravity-gradient, and orbital acceleration measurements

15. NUMBER OF PAGES
27

16. PRICE CODE
A03

17. SECURITY CLASSIFICATION OF REPORT	18. SECURITY CLASSIFICATION OF THIS PAGE	19. SECURITY CLASSIFICATION OF ABSTRACT	20. LIMITATION OF ABSTRACT
Unclassified	Unclassified		